Control of an Electrostatic MEMS Using Static and Dynamic Output Feedback

D. H. S. Maithripala[1], Jordan M. Berg[2] and W. P. Dayawansa[3]
Texas Tech University
{sanjeeva.maithripala,jordan.berg,wdayawan}@ttu.edu

Abstract

This paper examines control strategies for electrostatically-actuated MEMS, with the goal of using feasible measurements to eliminate the pull-in bifurcation, robustly stabilize any desired operating point in the capacitive gap, decrease settling time, and reduce overshoot. Towards these ends, we apply several approaches from the nonlinear control literature. Input-output linearization, passivity-based design, and the theory of port-controlled Hamiltonian systems lead naturally to static output feedback of device charge. This conclusion formalizes and generalizes several previously reported results from the MEMS literature. However, further application of these techniques suggests fundamental limitations of static charge feedback with regard to device performance. In particular, our analysis suggests that significantly improving transient behavior in lightly-damped MEMS requires dynamic estimation of the electrode velocity. We implement such estimation using a reduced-order nonlinear observer. Simulations predict greatly improved transient behavior, and large reductions in control voltage.

1 Introduction

Electrostatic actuation of microelectromechanical systems (MEMS) makes use of the attractive coulomb forces that develop between capacitively-coupled conductors differing in voltage. Electrostatically-actuated MEMS are popular because they are simple in structure, flexible in operation, and may be fabricated from standard, well-understood, materials [16]. However, it has long been recognized [28] that a saddle-node bifurcation called "snap-through" or "pull-in" is associated with electrostatic actuation, and results in operational limitations [5, 8, 35, 39]. Analysis of pull-in instabilities have been extended to rigid electrodes of complex geometry by Nemirovsky and Bochobza-Degani [29], and to flexible membranes by Pelesko and Triolo [32]. Bi-stable devices have been designed to exploit the bifurcation [13, 26, 3, 25, 7], however eliminating the effect would allow for enhanced functionality in applications including optical switching [7, 9, 10]; spatial light modulators for image projection [13] or data storage and image recognition [12]; and reconfigurable diffraction gratings for biosensors [46]. Specifically, eliminating pull-in can increase the range of the movable electrode by a factor of three, reduce the need for motion limiters and anti-stiction measures, and prevent disturbances from causing the movable electrode to depart from its stable operating region. Even when pull-in is the nominal behavior, device lifetimes are often limited by the incremental surface damage done at each contact [25]. To prevent pull-in during analog set-point operation with constant voltage bias, the nominal capacitive gap must be at least three times larger than the required range of motion. The result is a more difficult fabrication, and higher power requirements. Also, the region of attraction of the equilibrium point may be quite small, particularly near the bifurcation point. We wish to find a voltage control law that can be used to stabilize any equilibrium point in the gap, and to provide a large region of attraction. It is also desirable to keep the required control voltages small. Further discussion of pull-in may be found, for example, in [8, 29, 32, 39, 35].

Chu and Pister proposed closed-loop voltage control based on the electrode gap [8]. They show by analysis, and verify through simulation, that linear position feedback may be used to locally stabilize any point in the gap. Their implementation relies on local set-point control, and moves the electrode through large translations using a series of small step changes. Further, they do not address the nature of the position measurement. A well-known result due

[1]Department of Mechanical Engineering
[2]Department of Mechanical Engineering
[3]Department of Mathematics and Statistics

to Seeger and Crary is that every point in the gap may be stabilized by an appropriately sized capacitor placed in series with the electrostatic MEMS [35]. The analysis was later extended to include discussion of parasitics and the rotational *tip-in* instability for rigid electrodes [5, 29], and for membrane electrodes [32]. From a control perspective, capacitive stabilization implements static charge feedback, and can be shown to semi-globally stabilize every point of the gap [19, 20]. Several researchers have noted that the bifurcation associated with voltage control disappears when charge is considered as the control input instead of voltage. Furthermore, the high control voltages associated with capacitive stabilization are no longer required. Charge control has been most directly exploited by Nadal-Guardia, et al., who present open- and closed-loop switching circuits for injecting and maintaining the appropriate amount of charge on the device [27]. This scheme is globally stabilizing but does not address transient behavior. A version of charge control, implemented by means of a switched capacitor circuit is used by Seeger and Boser to stabilize a double-sided electrostatic MEMS [36], and an electrostatic MEMS with both rotational and translational degrees of freedom [37]. This method extends the operational range of the device, but guaranteed stability properties are only local.

Other control schemes presented in the literature include an inductor placed in series with the electrostatic MEMS [18]. This approach applies a sinusoidally-varying open-loop control voltage, and requires large time-scale separation between the mechanical and electrical subsystems. Its main advantage is a low control voltage requirement.

The above-cited papers are concerned only with *stabilization*. Transients are fixed by the physical damping of the mechanical subsystem, which for MEMS can vary widely. This can be seen, for example, by comparing the highly damped TI DMD mirrors [26] to the lightly damped structures reported in [25, 6]. As will be seen, the above stabilization strategies cannot significantly alter this damping. A major contribution of the current paper is to show that dynamic output feedback may be used to stabilize any point of the gap *with good transient performance*, as characterized by fast settling times and low overshoot for trajectories that start from equilibrium points in the gap. Improved transient performance of a MEMS device has been addressed by Wang for a PDE model of a cantilever beam with double-sided actuation [43]. Wang applies an energy-based control method and finds that a velocity feedback term is needed. Recognizing the difficulty of obtaining a velocity measurement, Wang uses a robust variable-structure approach. In this paper we also determine that velocity feedback is required for significant performance improvement, and propose a nonlinear velocity estimation scheme for dynamic output feedback control.

MEMS exhibit complex dynamical behavior [22, 23, 29, 33], but significant insight can be gained using a relatively simple nonlinear 1-D model [39]. Section 2 presents a model of an electrostatic MEMS with one mechanical translational degree of freedom. The model consists of a parallel plate capacitor with the top plate movable and the bottom plate fixed. The top plate is attached to flexible supports, modeled here by linear springs. Dynamically, our model assumes viscous damping, approximating structural and squeeze film effects. Stiction, electrical shorting, and other possible physical behaviors are neglected. Parameter variations, parasitic capacitance, and electrical noise are included in our simulations. The measured outputs are the voltage across the electrodes, and either the charge or the capacitance of the device. While the measurement of the velocity of the movable electrode is possible in the laboratory [41], this velocity is extremely difficult to sense directly during normal operation of the device. Thus we assume that the velocity of the movable electrode cannot be measured. Several structural considerations are important for nonlinear control design. In Section 2 we also examine key properties for the electrostatic MEMS model. We show that the model is naturally in *zero dynamics normal form*, and also that it has *port-controlled Hamiltonian with dissipation* (PCHD) structure. We show that the system is uniform relative degree one, compute the zero dynamics, and show that, under reasonable assumptions on electrode contact, they are weakly minimum phase.

In Section 3 we investigate four control strategies. We begin by exploiting the zero dynamics normal form, and applying input-output linearization. While input-output linearization typically requires full-state feedback, static output feedback suffices for the model under study. The first control design considers both linear and nonlinear static output feedback for stabilization of the observable dynamics of the linearized system. This additional feedback term will be a function only of charge. We have previously shown that the results of [27] in effect implement this strategy [19]. Here the mechanical subsystem corresponds exactly to the zero dynamics, and hence is unobservable in the input-output linearized system. Therefore this technique is not able add damping to the mechanical subsystem, and lightly damped MEMS will experience large overshoots and long settling times. Since the designs of [27] have this structure, they are constrained by this inherent performance limitation; a fact which those researchers observe experimentally.

Next, following the "almost linearized" approach of [17], we apply linear full-state feedback to the input-output

linearized system. While no global properties can be guaranteed—due to the effect of the neglected nonlinearities—performance of such a design is often good. Electrode velocity is among the quantities used in the control. This design approach is similar in some ways to the results of [36, 37], in which a nonlinear feedback of electrode position and velocity is effectively added to the linear charge feedback term. This nonlinear term arises as a by product of the amplifier design in the switched capacitor circuit that generates the charge feedback and hence does not improve the transient behavior. This observation is supported by the simulations presented in [36, 37].

Third, we note that the nonlinear system satisfies the conditions of [4], and apply the method of feedback passivation. Here the system is first input-output linearized, then passivated, using nonlinear full-state feedback. The closed-loop system is then controlled using a passivity-based technique called damping injection [38, 42]. Again, electrode velocity is required. Passivity-based techniques are known to be extremely robust to parameter variations and unmodelled dynamics in the sense that extremely large perturbations may be tolerated, as long as the perturbed system remains passive [15, 38, 42]. Many physical effects obey this restriction.

Finally, we apply energy shaping, exploiting the PCHD structure. Prior to input-output linearization, the system is not suitable for this method, but somewhat surprisingly the linearized system is. A cancellation occurs in the composite control with the result being that application of PCHD-based energy shaping to the linearized system is exactly charge feedback. It was shown in [19] that this generalizes the capacitive stabilization discussed in [35]. A critical observation about the resulting structure is that the dissipation term in the PCHD structure affects only the electrical subsystem. Hence it is not possible to inject significant additional damping into the mechanical subsystem, and transient performance is limited by the open-loop properties. Examination of the PCHD form shows that this is a structural problem, and not dependent on the choice of controller. Thus the nonlinear designs considered fall into two categories. One set, which can be implemented using static output feedback, and includes most of the previously reported stabilization results from the MEMS literature, can provide global or semi-global stabilization of any equilibrium point in the gap, but cannot improve the transient behavior of lightly damped systems. The other set can be used to improve transient performance, but electrode velocity is required, and hence implementation with a static controller is not possible.

This need for velocity in the control is addressed in Section 4, where we construct a dynamic observer for electrode velocity, using as measurements the voltage across the electrodes and either charge or the capacitance of the plates. The observer is based on standard nonlinear techniques, as described, for example in [17, 14]. The order of the observer is reduced from three states to one, following [44]. This simplifies implementation and improves performance. This observer is used to implement the two velocity-dependent state feedback laws. We prove in the Section that the domain of attraction is not reduced using the observer. Simulations show these controllers to have excellent performance, even in the presence of parameter variations, parasitic capacitance and measurement noise.

The present paper does not consider rotational degrees of freedom, or the associated tip-in bifurcation. These aspects are discussed in [22], and will be the subject of a more extended treatment in the future. Future work will also address parasitic capacitance, and the "charge pull-in" instability. Other interesting electrostatic MEMS configurations, such as higher degree-of-freedom rigid mirrors [22, 24, 34], or deformable membrane devices [33], display similar qualitative behavior to that described by the model considered here, and similar controllers have proven effective for those cases as well [22, 23]. A recent paper applies sliding-mode control to an electrostatically-actuated torsional mirror [34]. Sliding-mode techniques are a promising approach to MEMS control, but differ inherently from the continuous controls treated here. We believe that these are complementary points of view, both meriting further investigation.

2 The Open-Loop Model

A typical one dimensional model of an electrostatic microactuator is schematically represented in figure 1. The system is actuated by controlling the input voltage $v(t)$. The spring and dashpot represent the flexibility and damping in the support assembly. Let $Q(t)$ be the charge of the device, $i(t)$ the current through the resistor, $l(t)$ the air gap, $v(t)$ the input voltage, l_0 the zero voltage gap, A the plate area, m the mass of the movable electrode and ϵ the permittivity in the gap. Then the capacitance of the device is equal to $\epsilon A/l(t)$, the attractive electrostatic force on the top plate is $\frac{Q(t)^2}{2\epsilon A}$, and the current through the input resistance r is

$$i(t) \;=\; \frac{1}{r}\left(v(t) - \frac{Q(t)l(t)}{\epsilon A}\right).$$

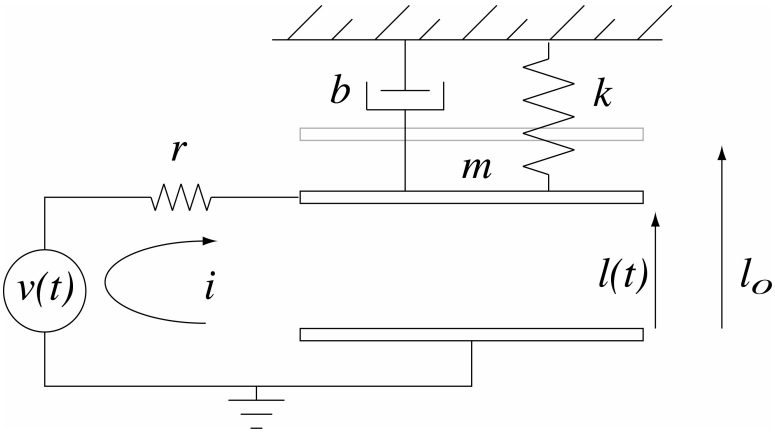

Figure 1: 1D model of a electrostatic microactuator. Top plate of the MEMS is free to move and the bottom plate is held fixed.

Such a simplified model was applied successfully in one of the earliest electrostatic MEMS applications [28], and is still used extensively. Here we use the equations of motion in the form given by Senturia [39],

$$m\ddot{l}(t) = -b\dot{l}(t) - k(l(t) - l_0) - \frac{Q^2(t)}{2\epsilon A}, \tag{1}$$

$$\dot{Q}(t) = \frac{1}{r}(v(t) - \frac{Q(t)l(t)}{\epsilon A}). \tag{2}$$

The state space of the system is $\{[Q(t), l(t), \dot{l}(t)]^T \in \mathcal{R}^3 \mid l \geq \delta_0\}$. Here δ_0 is the thickness of an insulating layer coated on the bottom electrode. Such a layer is needed physically to prevent shorting in the event of electrode contact. It is also useful mathematically to prevent singularity. We require only $\delta_0 > 0$.

In general, the input current $i(t)$ and the voltage across the device, $Q(t)l(t)/\epsilon A$, are available for measurement. Since they differ only by the control voltage, which is assumed known, it suffices from a control theory perspective to consider only one of them. Here we assume voltage is measured. Accurate measurement of capacitance across the device, $\epsilon A/l(t)$, is also possible [1]. Then the charge on the device, $Q(t)$, can be inferred from voltage and capacitance measurements. In the remainder of this paper we assume this has been done, and treat electrode voltage and electrode charge as the system outputs. An alternative means of determining charge is to insert a fixed capacitor in series and measure the voltage across it. Direct measurement of electrode velocity is possible in the laboratory [41], but typically not feasible under operational conditions. In Section 4 we show how the velocity may be estimated from measured quantities. Let σ be a positive constant. Performing a normalizing time scale change of $\hat{t} = \sigma t$, define $v = r\sigma\beta u$, $\alpha = \epsilon A r\sigma$, $\beta = \epsilon A\sigma\sqrt{mr\sigma}$, and let the normalized state vector $x = [Q/\beta, l/\alpha, \dot{l}/\alpha]^T$. Then the control system can be put into the state space form,

$$\begin{bmatrix} \dot{x}_1 \\ \dot{x}_2 \\ \dot{x}_3 \end{bmatrix} = \begin{bmatrix} -x_1x_2 \\ x_3 \\ -2\tau\omega x_3 - \omega^2(x_2 - \hat{l}_0) - x_1^2/2 \end{bmatrix} + \begin{bmatrix} 1 \\ 0 \\ 0 \end{bmatrix} u, \tag{3}$$

$$y_v = x_1x_2, \tag{4}$$

$$y = x_1, \tag{5}$$

with the state space $\mathcal{X} = \{[x_1, x_2, x_3]^T \in \mathcal{R}^3 | x_2 \geq \delta\}$, y_v is the voltage across the device divided by the constant $r\sigma\beta$, and y is the charge on the electrodes divided by the constant β. Here $\omega_n^2 = k/m$, $2\tau\omega_n = b/m$, $\omega = \frac{\omega_n}{\sigma}$,$\hat{l}_0 = l_0/\alpha$, and $\delta = \delta_0/\alpha > 0$.

For the purpose of global and semi-global stability analysis we assume that when the electrodes are in contact the system dynamics are governed only by the electrical subsystem, and that when the spring force acting on the electrode exceeds the electrostatic force the system switches back to its unconstrained form prior to contact. Formally, we have the following assumption:

Assumption 1 *The velocity of the moving electrode before and after contact satisfy the relation* $x_3^+ = -\mu x_3^-$ *where* $0 \leq \mu \leq 1$ *and* x_3^-, x_3^+ *are the velocities of the moving electrode just before and after contact respectively. When the system is restricted to the boundary of* $\mathcal{X}$, $\partial\mathcal{X} = \{[x_1, x_2, x_3]^T \in \mathcal{X} \mid x_2 = \delta\}$ *and (i) if* $x_1^2 \geq 2\,\omega^2(\hat{l}_0 - \delta)$, *the system is governed by* $\dot{x}_1 = -x_1 x_2 + u$, $\dot{x}_2 = 0$, $\dot{x}_3 = 0$, *or (ii) if* $x_1^2 < 2\omega^2(\hat{l}_0 - \delta)$ *the system switches back to (3).*

Effective approaches to nonlinear control require consideration of system structure. Often the first step in controller design is the transformation of the system into a particular normal form. Here we discover that the system model already naturally takes two such forms. The first is the *zero dynamics normal form*, associated with input-output linearization. The second is the *port-controlled Hamiltonian with dissipation* (PCHD), associated with energy-shaping. PCHD systems are passive if the Hamiltonian is bounded from below. Systems in zero dynamics normal form can be made passive if they are uniform relative degree one and their zero dynamics are weakly minimum phase [4]. We further discuss these normal forms in the following Section. They are used for controller design in Section 3.

2.1 Zero Dynamic Normal Form and the Stability of the Zero Dynamics

Consider the output $y = h(x) = x_1$. Then the system has uniform relative degree one, and further is naturally in the globally defined zero dynamic form of

$$\dot{y} = L_f h + L_g h\, u, \tag{6}$$
$$\dot{z} = q(z, y), \tag{7}$$

where $z = [z_1,\ z_2]^T = [x_2,\ x_3]^T$, $L_f h = -x_1 x_2$, $L_g h = 1$ and

$$q(z,y) = \begin{bmatrix} z_2 \\ -2\tau\omega z_2 - \omega^2(z_1 - \hat{l}_0) - y^2/2 \end{bmatrix}$$

if $x \notin \partial\mathcal{X}$ and $q(z, y) = [0\ 0]^T$ if $x \in \partial\mathcal{X}$. The zero dynamic subsystem (7) can thus be thought of as a switched system, where switching occurs when the electrodes come into contact.

Consider the constrained system $y \equiv \bar{x}_1$. The point $[\bar{x}_2,\ 0]^T$ is an equilibrium of the constrained or zero dynamic system. Observe that for any $\delta < \bar{x}_2 < \hat{l}_0$, $\bar{x}_1^2 = 2\omega^2(\hat{l}_0 - \bar{x}_2) < 2\omega^2(\hat{l}_0 - \delta)$, and thus from assumption 1 we have that the radially unbounded quadratic positive definite function $W(z) = \omega^2\,(z_1 - \bar{x}_2)^2/2 + z_2^2/2$ is a common Lyapunov function for the switched system (7). This implies that the zero dynamics are weakly minimum phase, as required by [4]. Therefore, the equilibrium $\bar{z} = [\bar{x}_2,\ 0]^T$ of the zero dynamics, $\dot{z} = q(z, \bar{x}_1)$, is globally asymptotically stable [11]. The dynamics of (7) are exactly those of the mechanical subsystem. The zero dynamics have the property that they are unobservable when the output is identically equal to its constrained value [14]. Therefore the dynamics of the mechanical subsystem are decoupled from the output when the constraint is attained, and so output feedback cannot be used to improve the open-loop mechanical damping.

Since the system given by (6)–(7) with output $y = h(x) = x_1$ has uniform relative degree one, the feedback control law defined by

$$u = -[L_g h]^{-1}(L_f h - \hat{u}) \tag{8}$$

is globally smooth. Substituting the smooth feedback law (8) in (6)–(7) we obtain the following input-output linearized system

$$\dot{y} = \hat{u}, \tag{9}$$
$$\dot{z} = q(z, y). \tag{10}$$

Since $L_f h = -y_v(t)$ is measured, it is possible to linearize the original system using static output feedback.

2.2 PCHD Structure

The system (3)–(4) has a PCHD structure. That is, it can be expressed as

$$\dot{x} = [J(x) - R(x)]\,\frac{\partial H}{\partial x} + g(x)\,u, \tag{11}$$
$$y_d = g(x)^T\,\frac{\partial H}{\partial x}. \tag{12}$$

where J is skew-symmetric and R is positive semi-definite. In this case,

$$J(x) = \begin{bmatrix} 0 & 0 & 0 \\ 0 & 0 & 1 \\ 0 & -1 & 0 \end{bmatrix}, \quad R(x) = \begin{bmatrix} 1 & 0 & 0 \\ 0 & 0 & 0 \\ 0 & 0 & 2\tau\omega \end{bmatrix}, \quad g(x) = \begin{bmatrix} 1 \\ 0 \\ 0 \end{bmatrix}$$

The function $H(x)$ is the total energy or Hamiltonian function given by

$$H(x) = \frac{1}{2}x_1^2 x_2 + \frac{1}{2}\omega^2(\hat{l}_0 - x_2)^2 + \frac{1}{2}x_3^2, \tag{13}$$

and $\frac{\partial H}{\partial x}$ is the column vector consisting of the partial derivatives of $H(x)$. $J(x)$ captures the internal interconnection structure, $g(x)$ captures the external interconnection with the environment and $R(x)$ captures the damping structure of the system [31, 42]. The input u and the output y_d are called the power port variables and their product has units of power. Observe that $y_d = y_v$ is the voltage across the device and is a measured output. For a given y_v there exist two equilibria in the gap, and therefore the system with this output is not zero state detectable to any one of the equilibria. This precludes use of voltage as the output to stabilize any equilibrium and inject damping.

Usually the process of input-output linearization destroys the PCHD property. However in this case it does not. The PCHD structure of the input output linearized system (9) – (10) is given by,

$$J_i(x) = \begin{bmatrix} 0 & 0 & 0 \\ 0 & 0 & 1 \\ 0 & -1 & 0 \end{bmatrix}, \quad R_i(x) = \begin{bmatrix} 0 & 0 & 0 \\ 0 & 0 & 0 \\ 0 & 0 & 2\tau\omega \end{bmatrix}, \quad g_i(x) = \begin{bmatrix} 1 \\ 0 \\ 0 \end{bmatrix}$$

and $H_i(x) = H(x)$. The only difference with the non input-output linearized case is in the R matrix.

3 Stabilization Strategies

In this section we investigate the stabilization of a desired equilibrium $\bar{x} = [\bar{x}_1, \quad \bar{x}_2, \quad 0]^T$. Given any desired equilibrium gap, $\bar{x}_2$, an obvious and natural question is whether there exists a locally stabilizing observer-based controller that is based on the linear approximation of the system. The answer is yes, provided $\bar{x}_2 \neq \hat{l}_0$. In fact, it is even possible to design a first-order reduced-order observer. However simulations show that the region of attraction of the locally stabilized origin is quite small, especially if the stabilized gap is small and the control gains are high [19]. Thus we investigate the existence of globally or semi-globally stabilizing nonlinear feedback control laws.

In the remaining parts of this Section, we investigate four control strategies. We begin by exploiting the zero dynamics normal form, and applying input-output linearization. Once the system has been input-output linearized, the only observable dynamics are those of charge. Our first design considers both linear and nonlinear static output feedback, for stabilization of the observable dynamics. This stabilizes the entire system since the zero dynamics are weakly minimum phase. We show that any point in the gap may be globally stabilized, but as mentioned earlier, the mechanical damping cannot be improved. We have previously shown that the results of [27] in effect implement this strategy [21].

The input-output linearized system is a linear map from input to output, but due to the nonlinear zero dynamics it is still a nonlinear system. A general technique for using linear ideas to improve the overall system performance is to apply linear full-state feedback. The feedback is computed for the system obtained by linearizing the zero dynamics about a desired operating point—this is the "almost linear" approach of Krener [17]. While no global properties can be guaranteed, due to the effect of the neglected nonlinearities, performance of such a design is often good. However, electrode velocity is used in the control, and so must be estimated. The work of [36, 37] uses a very similar method, but their approach heavily stresses fabrication, and their feedback function is highly restricted by the circuitry design they choose to implement it. As presented, their design is not capable of improving the damping of the mechanical subsystem, and they note in their experiments that lightly damped structures exhibit large overshoot under closed-loop control.

Third, we note that the nonlinear system satisfies the conditions of [4], and apply the method of feedback passivation. Here the system is first input-output linearized, then passivated, using nonlinear full-state feedback. The closed-loop system is then controlled using any one of several passivity-based approaches. However, the feedback passivation step uses electrode velocity, so once again an estimator is required.

Finally, we exploit the PCHD structure. PCHD-based energy shaping is a powerful technique for stabilizing a desired point by minimally modifying the natural system behavior. the approach requires the existence of a certain class of system invariants called Casimirs. Unfortunately, while the model (3)–(5) is in PCHD form, it does not have any suitable Casimirs. However, after input-output linearization, not only does the system retain PCHD form, but it now has the necessary Casimirs. Now application of PCHD-based energy shaping is exactly charge feedback, equivalent to the capacitive stabilization discussed in [35]. This requires only static output feedback, but the damping of the mechanical subsystem cannot be improved. Examination of the PCHD form shows that this is a structural problem, and not dependent on the choice of controller.

3.1 Input-Output Linearization Plus Charge Feedback

We note that the input-output linearized system given by (9)–(10) can be considered as the interconnection of two subsystems, where $q(y,z)$ takes the form $q(z,y) = q(z,\bar{x}_1) + s(y)$. Since, for any given desired equilibrium $\bar{x}$ the point $[\bar{x}_2,\ 0]$ of the zero dynamic subsystem given by $\dot{z} = q(z,\bar{x}_1)$ is globally asymptotically stable and $W(z) = \omega^2\,(z_1 - \bar{x}_2)^2/2 + z_2^2/2$ satisfies $L_{q(z,\bar{x}_1)}\,W \leq 0$, Theorem 4.7 of [38](page 129) guarantees that any feedback $\hat{u} = \psi(y)$ that globally asymptotically and locally exponentially stabilizes the forced equilibrium $\bar{x}_1$ of (9), globally asymptotically stabilizes the equilibrium $\bar{x} = [\bar{x}_1,\ \ \bar{x}_2,\ \ 0]^T$ of (9)–(10). Thus

$$u = y_v + \psi(y). \tag{14}$$

globally asymptotically stabilizes the forced equilibrium $\bar{x} = [\bar{x}_1,\ \ \bar{x}_2,\ \ 0]^T$ of (6)–(7). One obvious choice for ψ is $\psi(y) = -k_q\ (y - \bar{x}_1)$. However observe that the gap dynamics include the zero dynamics corresponding to the mechanical subsystem, and hence these charge feedback schemes suffer from long settling times and large overshoots if the natural damping is low. We have shown in [19] that the current drive method proposed in [27] is also equivalent to control with respect to the input-output linearized system (9)–(10). In [22] we generalize the approach of input-output linearization followed by charge feedback to the general stabilization problem of a 6-DOF rigid electrostatically-actuated device. We only require that the system is uniform relative degree one and weakly minimum phase. Thus this scheme should guarantee global asymptotic stability in the presence of unmodelled mechanical perturbations that preserve these properties. Examples of such effects include small parameter variations, fluid damping and nonlinear spring terms.

3.2 Linear State Feedback Controller

Observe that the system (9)–(10) is linearly controllable at any $\bar{x}$ such that $\bar{x}_2 \neq \hat{l}_0$. Thus it is possible to find an F such that the linear feedback control $\hat{u} = F(x - \bar{x})$ locally asymptotically stabilizes the forced equilibrium $\bar{x}$ of (9)–(10) with arbitrarily fast dynamics close to $\bar{x}$. For a generic $F = [f_1\ \ f_2\ \ f_3]$ it is seen that the system has two equilibria. Thus this scheme can not globally stabilize the system. However with $f_2 = 0$, $\bar{x}$ is the only equilibrium of the system and the Routh-Hurwitz test shows that all the eigenvalues of the linearized system lie in the strict left half complex plane for all $f_1 < 0$ and $f_3 > 0$ (the characteristic polynomial of the linearized system matrix is $\lambda^3 + (2\tau\omega - f_1)\lambda^2 + (\omega^2 - 2f_1\tau\omega + \kappa)\lambda - f_1\omega^2$ where $\kappa = \bar{x}_1 f_3$). Setting $f_1 = -k_l$, for some fixed positive k_l, and with the aid of the root locus with respect to the gain κ it is possible to select the feedback gain f_3 such that good transients are achieved for low damping. Setting $f_3 = 0$ yields the globally stable linear charge feedback law, whose transient response depends on the damping of the mechanical system. Thus in the case of low damping improved transient performance requires that f_3 be nonzero. For a suitably designed k_l and f_3 simulations indicate that the system has good transient performance as well as a large region of attraction. Explicitly this control law is expressed by

$$u = \varphi_2(y_v, y, x_3) = y_v + \frac{\kappa}{\bar{x}_1} x_3 - k_l(y - \bar{x}_1), \tag{15}$$

and locally asymptotically stabilizes the point $\bar{x} = [\bar{x}_1\ \ \bar{x}_2\ \ 0]^T$ of (3). Although this control law exhibits very good performance and stability properties, its implementation requires the measurement of the velocity variable x_3. In Section 4 a reduced-order dynamic observer is constructed to estimate x_3 with arbitrary linear error dynamics.

3.3 Feedback Passivation

In Section 2.1 we showed that the system (3) has uniform relative degree one and weakly minimum phase zero dynamics. Then, as shown in [4], the system is feedback equivalent to a passive system. The constructive proof of [4] is adopted in [38] as a design methodology for the passive feedback interconnection of subsystems. The first step in this process is to input-output linearize the system. Thus we begin with the input-output linearized system (9)–(10). It can be considered as the interconnection of two subsystems. System (10) can be expressed as $\dot{z} = q(z,\bar{x}_1) + r(y)(y - \bar{x}_1)$, where $r(y) = [0\ \ -(y - \bar{x}_1)/2]^T$ and $q(z,\bar{x}_1)$ describes the zero dynamics with respect to $y \equiv \bar{x}_1$. Since the zero dynamics are weakly minimum phase, there exists an $S_2(z)$ such that $L_q S_2 \leq 0$. In this case

the zero dynamics correspond exactly to the forced mechanical subsystem, and the total energy of the mechanical subsystem is one suitable choice for S_2, $S_2(z) = \omega^2(z_1 - \bar{x}_2)^2/2 + z_2^2/2$. System (9) is passive with storage function $S_1(y) = (y - \bar{x}_1)^2/2$ and output y. Now consider the function $S(y,z) = S_1(y) + S_2(z)$. Taking the time derivative of $S(y,z)$ along the trajectories of (9)–(10) gives

$$\dot{S} = L_q S_2(z) + (L_{r(y)} S_2(z) + \hat{u})(y - \bar{x}_1).$$

Thus the feedback $\hat{u} = -L_{r(y)} S_2(z) + \hat{v}$ renders (9)–(10) passive with storage function $S(y,z) = S_1(y) + S_2(z)$, output y and input $\hat{v}$. The function $S(y,z)$ is globally proper and positive definite in $\mathcal{X}$. The closed-loop system is zero state detectable to $\bar{x}$ with the output $y = x_1$. Then damping control $\hat{v} = -k_p(y - \bar{x}_1)$ with $k_p > 0$ guarantees that $S(y,z)$ strictly decreases along the trajectories of (9)–(10). Therefore,

$$u = \varphi_1(y_v, y, x_3) = y_v + \frac{1}{2} x_3 \, (\bar{x}_1 + y) - k_p(y - \bar{x}_1) \tag{16}$$

globally asymptotically stabilizes the point $\bar{x} = [\bar{x}_1 \;\; \bar{x}_2 \;\; 0]^T$ of (3). Observe that this feedback is a function of the measured variables y_v, y and the unmeasured velocity variable x_3. In section 4 we construct a reduced-order dynamic observer to estimate x_3 with arbitrary linear error dynamics.

Passivity-based control is inherently robust to unmodelled dynamics and parameter variations that preserve passivity [15, 38, 42]. Although we do not rigorously characterize such perturbations in this paper, the simulation results presented in Section 4.1 support this observation. In [22] we show that this intuitive controller can be naturally extended to a 6-DOF electrostatically-actuated rigid MEMS.

3.4 Charge Feedback

In this section we present stabilizing feedback control strategies from a passivity point of view. A nonlinear control system is said to be *passive* with storage function $S(x)$ if there exists a smooth positive semidefinite function $S(x)$ such that the inequality $S(x(t)) - S(x(0)) \leq \int_0^t u^T y \, d\tau$ holds for all admissible $u(\cdot)$. The advantage of passivity is that stabilization can be achieved by static output feedback of the system and the storage function is a candidate for a Lyapunov function of the system [30, 15]. To illustrate this point consider the following. If $S(x)$ is differentiable, $\dot{S}(x)) \leq u^T y$, and so, if $S(x)$ is positive definite, radially unbounded, and $S(\bar{x}) = 0$, then the static output feedback $u = -y$ makes the $\bar{x}$ globally asymptotically stable, with $S(x)$ as a Lyapunov function. The problem with applying this method is finding a suitable $S(x)$. In general for physical problems total energy is a good candidate, however it may require some further *shaping* [2, 31, 42]. If the system has a PCHD structure then [31, 42] provide a way of shaping the total energy of the system such that the shaped energy qualifies as a suitable Lyapunov function. This is achieved by looking for the *Casimir* functions, $C_i(x)$, that satisfy $\frac{\partial C_i}{\partial x}^T [J - R] = 0$. Any constant is automatically a Casimir; non-constant Casimirs are said to be *nontrivial*. They are the invariant quantities of the uncontrolled trajectories of the PCHD system for any Hamiltonian. If nontrivial Casimir functions $C_i(x)$, for $i = 1, 2, 3, \cdots, m$ exists then any function of the form $H_a(C_1(x), C_2(x), \cdots, C_m(x))$ is used to shape the Hamiltonian $H_c(x)$ such that it is positive definite in some neighborhood of $\bar{x}$. Once this has been achieved the damping control $u = -y_c$ locally asymptotically stabilizes the forced equilibrium $\bar{x}$ of (11) provided the system with the output $y_c = g^T \frac{\partial H_c}{\partial x} = y_v(t) + \frac{\partial H_a}{\partial x}$ satisfies a detectability condition.

It is seen that the PCHD structure of (3) does not admit any non-trivial Casimir functions. In the case of the input output linearized system (9) – (10) it is straight forward to see that the only non trivial Casimir functions of the PCHD are of the form $C_i(x_1)$. Thus the shaping of the Hamiltonian will have to be achieved only with functions of the form $H_a(x_1)$. If $H_c(x) = H(x) + H_a(x_1)$ is positive definite locally (globally) proper and the system (11) is zero state detectable to $\bar{x}$ with respect to the output $y_c = y_v + \frac{\partial H_a}{\partial x_1}$ then the feedback $\hat{u} = -y_c = -y_v(t) - \frac{\partial H_a}{\partial x_1}$ locally (globally) stabilizes the forced equilibrium $\bar{x}$ of (9) – (10). Observe that this control results in $u = -\frac{\partial H_a}{\partial x_1}$ with respect to the original system (3). Therefore with respect to the original system (3) the feedback $u = -\frac{\partial H_a}{\partial x_1}$ locally (globally) asymptotically stabilizes the $\bar{x}$ and hence this approach necessarily results exactly in charge feedback with respect to (3).

It can be shown that a necessary and sufficient condition for $H_c(x)$ to be positive definite in some neighborhood $\mathcal{U}$ of $\bar{x} = [\bar{x}_1, \;\; \bar{x}_2, \;\; 0]^T$, for any $\delta < \bar{x}_2 < \hat{l}_0$, is that $\frac{\partial H_a}{\partial^2 x_1}^2(\bar{x}_1) > 2\hat{l}_0 - 3\delta$. A necessary and sufficient condition for the detectability condition is that the only solution, in $\mathcal{U}$, of the set of equations

$$x_3 \;\; = \;\; 0 \tag{17}$$

$$x_1 x_2 + \frac{\partial H_a}{\partial x_1}(x_1) = 0 \quad (18)$$

$$x_1^2 - 2\omega^2(\hat{l}_0 - x_2) = 0 \quad (19)$$

be $\bar{x} = [\bar{x}_1,\ \bar{x}_2,\ 0]^T$. Thus if it is possible to find $H_a(x_1)$ satisfying these conditions then the control

$$u = -\frac{\partial H_a}{\partial x_1}, \quad (20)$$

locally asymptotically stabilizes the origin of (3). In the case where H_c is positive definite, radially unbounded and the input-output linearized system is zero state detectable to $\bar{x}$ with output y_c then the control law globally asymptotically stabilizes $\bar{x}$.

Following this it is shown in [19] that

$$u = \bar{x}_1\bar{x}_2 - k_c(y - \bar{x}_1) \quad (21)$$

semi-globally assymptotically stabilizes the origin of (3). We have shown also in [19] that this semi-globally stabilizing control law is equivalent to the capacitive feedback law of [35]. Also, $u = \bar{x}_1\bar{x}_2 - k_1(y-\bar{x}_1) - k_2(y-\bar{x}_1)^3$ will globally asymptotically stabilize any equilibrium if $k_1 = \gamma 2(\hat{l}_0 - 3\delta)$, $\gamma > 1$ and $k_2 > \frac{2(4\gamma+1)}{(2\gamma+1)}$ [19].

The Casimir functions $C_i(x_1)$ of the PCHD system satisfy the additional condition that $\frac{\partial C_i}{\partial x}J = 0$ and $\frac{\partial C_i}{\partial x}R = 0$. In such a case it is straightforward to show as shown in [31, 42] that the closed-loop system is also a PCHD system with Hamiltonian $H_c(x)$, interconnection matrix J and damping matrix $R + gg^T$. In this case the only nonzero element of $g\,g^T$ is the first diagonal element. Thus this scheme adds damping only in the electrical part of the system.

4 Dynamic Output Feedaback

Observe that the system (3) with output $\hat{y} = [y\ \ y_v/y]^T$ can be expressed as

$$\dot{x} = \hat{A}x + \Gamma(\hat{y}) + Bu \quad (22)$$

$$\hat{y} = Cx. \quad (23)$$

where

$$\hat{A} = \begin{bmatrix} 0 & 0 & 0 \\ 0 & 0 & 1 \\ 0 & -\omega^2 & -2\tau\omega \end{bmatrix}, \quad \Gamma(\hat{y}) = \begin{bmatrix} 0 \\ 0 \\ -\frac{y^2}{2} \end{bmatrix},$$

$$B = \begin{bmatrix} 1 \\ 0 \\ 0 \end{bmatrix}, \quad C = \begin{bmatrix} 1 & 0 & 0 \\ 0 & 1 & 0 \end{bmatrix}.$$

A full-order observer with linear error dynamics can be designed for a system of the form (22)–(23) [14]. Further, since $(C, \hat{A})$ is observable, these dynamics can be made arbitrarily fast. For linear systems the order of a dynamic observer may be reduced by one for each measured output Wonham shows that such an order reduction improves performance of the linear observer in the sense of faster convergence, and reduced sensitivity to measurement noise [44]. Furthermore, implementation of the reduced-order observer will be simpler. Based on these arguments, we adapt the method of Wonham to construct a reduced-order *non-linear* observer with linear error dynamics:

$$\dot{z} = Tz + VK\hat{y} + V\Gamma(\hat{y}) + VB\hat{u}, \quad (24)$$

$$\hat{x} = W^{-1}\begin{bmatrix} \hat{y} \\ z \end{bmatrix}. \quad (25)$$

Where $z \in \mathcal{R}$ and $\hat{x}$ is the estimated state. The reduced-order observer parameters T, K and V are selected such that $W = [C^T\ V^T]^T$ is invertible, $V(\hat{A} - KC) = TV$ and the spectrum of T is pre-assigned [44] (that is $T < 0$). Setting $e = (Vx - z)$ a straightforward calculation shows that

$$\dot{e} = Te, \quad (26)$$

$$\hat{x} = x - W^{-1}D\,e, \quad (27)$$

where $D = [0\ \ 0\ \ 1]^T$. The vector $W^{-1}D$ is of the form $[0\ \ 0\ \ \vartheta]^T$ for some constant ϑ. Thus the velocity estimate is of the form $\hat{x}_3 = x_3 - \vartheta e$. We note that this observer design does not depend on the desired equilibrium point.

Implementing (16) with $u = \varphi_1(y_v, y, \hat{x}_3)$ and the observer (24) – (25) we have the closed-loop system

$$\dot{x} = \hat{A}x + \Gamma(\hat{y}) + B\,\varphi_1(y_v, y, x_3) - B\,\vartheta\,ex_1, \tag{28}$$

$$\dot{e} = Te. \tag{29}$$

Theorem 4.7 of [38] guarantees that the equilibrium point $[\bar{x}_1\ \ \bar{x}_2\ \ 0\ \ 0]^T$ of (28) – (29) is globally asymptotically stable.

Implementing (15) with $u = \varphi_2(y_v, y, \hat{x}_3)$ and the observer (24) – (25) we have the closed-loop system

$$\dot{x} = \hat{A}x + \Gamma(\hat{y}) + B\,\varphi_2(y_v, y, x_3) - B\,\vartheta\,\frac{\kappa}{\bar{x}_1}e, \tag{30}$$

$$\dot{e} = Te. \tag{31}$$

Thus the equilibrium point $[\bar{x}_1\ \ \bar{x}_2\ \ 0\ \ 0]^T$ of (30) – (31) is locally asymptotically stable.

4.1 Simulation Results

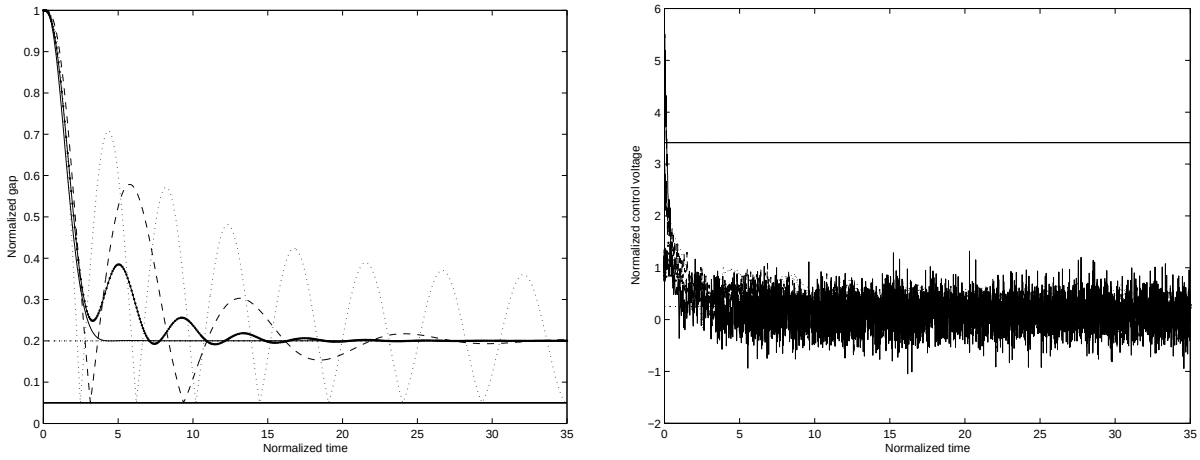

(a) Nominal system.

(b) System with parameter variations, measurement noise and parasitic capacitance.

Figure 2: Stabilizing a gap of 20% of the zero voltage gap. The system starts at equilibrium point (0 1 0). Solid curve: linear feedback (15), solid-dotted curve: passivity-based control (16), dashed curve: linear charge feedback (21), dotted curve: charge feedback with input-output linearized system (14).

This section presents simulations of the control schemes (14), (15), (16) using dynamic velocity estimation. Performance of the capacitive feedback (21) [35] is also included for comparison. The normalized natural frequency of the system is $\omega = 1$ and the damping ratio $\tau = 0$. The controller and observer parameters are chosen as follows: observer gain $T = -10$, control parameters $k_l = 4.3$ and $\kappa = 6.89$ for (15), control parameter $k_p = 0.8$ for (16), control parameter $k_q = 2.08$ for (14) and control parameter $k_c = 2.08$ for (21). A nominal gap of $\bar{x}_2 = 0.2$ is stabilized by each of these controls. Then $\bar{x}_1^2 = 1.6$.

Figures 2(a) and 3(a) show the displacement profiles and control response, respectively, for each of the controllers developed in this paper, as well as for the capacitive feedback method. Figures 2(b) and 3(b) show the displacement profile and control response, respectively, in the presence of parameter variations, measurement noise, and parasitic capacitance. Parameter variations were chosen to give a 2 % decrease in the natural frequency of the mechanical system, a 10 % increase in the damping, and a 1 % decrease in the electrode area. A parasitic capacitance equal to 10 % of the zero-voltage capacitance was added between the top electrode and ground. Measurement noise was additive, unity variance, white noise. The controllers derived in this paper perform quite satisfactorily, while the capacitive stabilization scheme is destabilized by these perturbations. A smaller control capacitance could have been used to stabilize this last method as well.

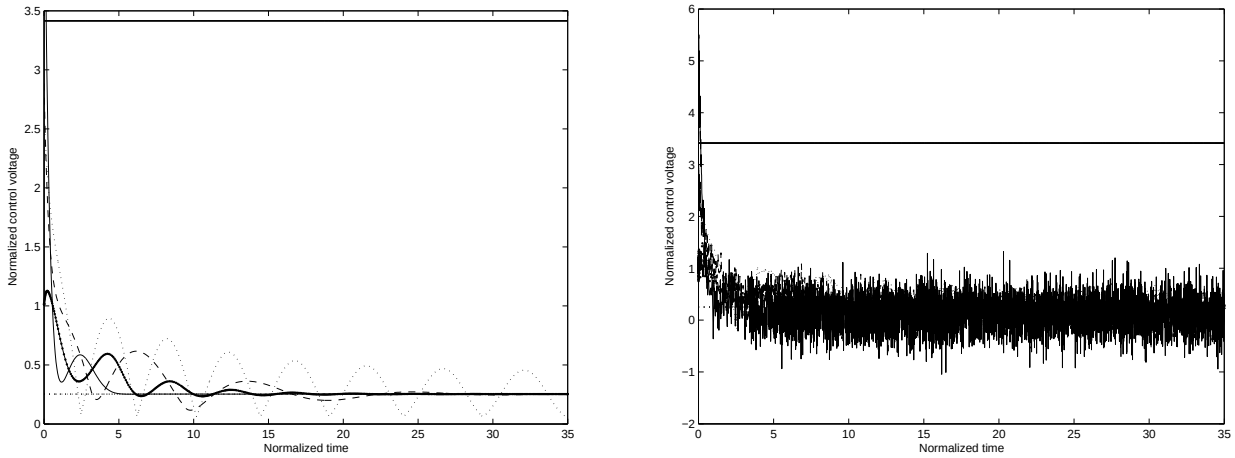

(a) Nominal system.

(b) System with parameter variations, measurement noise and parasitic capacitance.

Figure 3: The control voltage $u(t)$. The solid line at $u = 3.4$ corresponds to the series voltage source required by the series capacitor method. Solid curve: linear feedback (15), solid-dotted curve: passivity-based control (16), dashed curve: linear charge feedback (21), dotted curve: charge feedback with input-output linearized system (14).

Figures (2) shows that the locally stabilizing linear feedback control (15) performance is better than that of the passive based control (16). The advantage of the passivity-based controller is its global stability, and its guaranteed robustness to passivity-preserving perturbations. It is shown in [40] how to interpolate between a controller giving global asymptotic stability, and a controller giving good local performance. Such a method could be applied here, although the passivity-based robustness property may no longer be guaranteed.

5 Conclusions

We have considered a simple model of an electrostatic MEMS. We have assumed that the voltage across the device, and either the device charge or the device capacitance are available for measurement, and have used four approaches from the nonlinear control literature to address the problems of stabilization and improved transient response. Two of these approaches give static output feedback controllers, which generalize many results from the MEMS literature. Like these prior methods, they cannot improve the transient performance of the device, as quantified by shorter settling times, and decreased overshoot. The other two approaches, in conjunction with a reduced-order, nonlinear observer, give rise to dynamic output feedback controllers that both stabilize any equilibrium point, and improve performance. While the model used exhibits only one translational degree of freedom, the approach is systematic and generalizable.

Acknowledgement

The authors gratefully acknowledge the support of NSF grant ECS-0218245.

Nomenclature

A	=	Cross sectional area of each of the electrodes
b	=	Damping coefficient
H	=	Hamiltonian of the system
H_c	=	Controlled Hamiltonian
i	=	Current through the device
k	=	Linear spring constant
k_c	=	Capacitor charge feedback gain
k_l	=	Linear charge feedback gain
k_p	=	Passivity charge feedback gain
k_q	=	Input-output linearized charge feedback gain
l	=	The gap between the electrodes
l_0	=	Zero voltage gap
$\hat{l}_0$	=	Normalized zero voltage gap
m	=	Mass of the movable elctrode
Q	=	Charge on a electrode
r	=	Electrical resistance in the circuit
t	=	Time
$\hat{t}$	=	Normalized time
u	=	Normalized control voltage
v	=	Control voltage
x	=	Normalized state vector
x_1	=	Normalized charge
$\bar{x}_1$	=	Normalized desired equilibrium charge
x_2	=	Normalized gap
$\bar{x}_2$	=	Normalized desired equilibrium gap
x_3	=	Normalized velocity
$\mathcal{X}$	=	Constrained state space
y	=	Measured normalized charge ($y = x_1$)
y_v	=	Measured normalized voltage drop across the device
z	=	Normalized mechanical system states ($z = [x_2,\, x_3]^T$).
α	=	Gap normalizing constant
β	=	Charge normalizing constant
ϵ	=	Permittivity of the dielectric medium
δ	=	Insulation thickness of the bottom electrode
δ_0	=	Normalized insulation thickness of the bottom electrode
κ	=	Controller parameter
σ	=	Time normalizing constant
τ	=	normalized damping ratio
ω	=	Normalized mechanical natural frequency
ω_n	=	Mechanical natural frequency

References

[1] Ayela F., Bret J. L. , Chaussy J., Fournier T. and Menegaz E.,2000 , "A Two-Axis Micromachined Silicon Actuator with Micrometer Range Electrostatic Actuation and Picometer Sensitive Capacitive Detection," *Review of Scientific Instruments*, **71** (5), pp 2211–2218.

[2] Bloch A. M., Chang D. E., Leonard N. E. and Marsden J. E., 2001, "Controlled Lagrangians and the Stabilization of Mechanical Systems II: Potential Shaping," *IEEE Transactions on Automatic Control*, **46** (10), pp 1556 – 1571.

[3] Bloom D. M. 1997, "The Grating Light Valve: Revolutionizing Display Technology, " *Projection Displays III Symposium, SPIE Proceedings,* 3013.

[4] Byrnes C. I., Isidori A. and Willems J. C., 1991, "Passivity, Feedback Equivalence, and the Global Stabilization of Minimum Phase Nonlinear Systems," *IEEE Transactions on Automatic Control*, **36** (11), pp 1228 – 1240.

[5] Chan E. K. Dutton R. W. 2000, "Electrostatic micromechanical actuator with extended range of travel,", *Journal of Microelectromechanical Systems*, **9** (3), pp. 321–328.

[6] Larnaudie H. C., Rivoirard F. and Jammes B., 1999, "Analytical Simulation of a 1D Single Crystal Silicon Electrostatic Micromirror," *Proc. of the Second Int. Conf. on Modelling and Simulation of Microsystems, Semiconductors, Sensors and Actuators, Chicago, CA*, pp 628–631.

[7] Chu P. B. , Lee S., and Park S., 2002, "MEMS: The Path to Large Optical Crossconnects," *IEEE Communications Magazine*, pp 80–87.

[8] Chu P. B. and Pister S. J., 1994, "Analysis of Closed-loop Control of Paralle-Plate Electrostatic MicroGrippers," *Proc. of IEEE Int. Conf. Robotics and Automation*, pp 820–825.

[9] Chung S., and Kim Y., 1999, "Design and Fabrication of a 10×10 micro-spatial Light Modulator Array for Phase and Amplitude Modulation ," *Sensors and Actuators*, **78** pp. 63–70.

[10] Comtois J., Michalicek A., Cowan W., and Butler J., 1999, "Surface-micromachined Polysilicon MOEMS for Adaptive Optics," *Sensors and Actuators*, **78** pp. 54–62.

[11] Dayawansa W. P. and Martin C. F., 1999, "A converse Lyapunov Theorem for a Class of Dynamical Systems which Undergo Switching", *IEEE Trans. Automat. Control*, **44**, pp. 751–760.

[12] Florence J. M. and Gale R. O. 1988, "Coherent optical correlator using a deformable mirror device spatial light modulator in the Fourier plane," *Applied Optics*, **27** (11), pp. 2091–2093.

[13] Hornbeck L. J. 1998, "From cathode rays to digital micromirrors: A history of electronic projection display technology," *TI Technical Journal*, July–September, pp. 7–46.

[14] Isidori A., 1995, *Nonlinear Control Systems,* 3rd Ed., Springer-Verlag, London.

[15] Kelkar A. G., Joshi S. M. and Alberts T. E., 1995, "Passivity Based Control of Nonlinear Flexible Multibody Systems", *IEEE Trans. Automat. Control*, **40** (5), pp. 910–914.

[16] Kovacs G. T. A. 1998, *Micromachined Transducers Sourcebook,* McGraw-Hill, New York.

[17] Krener A. J., 1999, "Feedback Linearization," *Mathematical Control Theory*, pp 66–95, Springer-Verlag, New York.

[18] Kyynarainen J. M., Oja A. S. and Seppa H., 2001, "Increasing the Dynamic Range of a Micromechanical Moving-Plate Capacitor," *Journal of Analog Integrated Circuits and Signal Processing*, **29** pp. 61–70.

[19] Maithripala D. H. S., Berg J. M. and Dayawansa W. P., 2003, "Capacitive Stabilizatipon of an Electrostatic Actuator: An Output Feedback Viewpoint," *Proc. of the 2003 American Control Conference, June 4-6*, Denver, CO, pp. 4053–4058.

[20] Maithripala D. H. S., Berg J. M., and Dayawansa W. P., 2003, "An Energy Based Method for Stabilization of an Electrostatic Actuator," *Proc. of the IMECE*, Washington, DC.

[21] Maithripala D. H. S., Berg J. M. and Dayawansa W. P., 2003, "Nonlinear Dynamic Output Feedback Stabilization of Electrostatically-Actuated MEMS," *Proc. of the CDC*, Maui, HW.

[22] Maithripala D. H. S., Gale R. O., Holtz M. W., Berg J. M. and Dayawansa W. P., 2003, "Nano-precision control of micromirrors using output feedback," *To appear in the Proc. of the CDC*, Maui, HW.

[23] Maithripala S., 2003, "Nonlinear Control of an Electrostatically Actuated MEMS," *Ph. D. Thesis*, Texas Tech University, Texas.

[24] Maithripala D. H. S., Dayawansa W. P., and Berg J. M., 2003, "Intrinsic Observer-Based Control on Lie Groups," *SIAM Journal of Control and Optimization*, in review.

[25] McCarthy B. Adams G. G. McGruer N. E. and Potter D., 2002, ' 'A Dynamic Model, Including Contact Bounce, of an Electrostatically Actuated Microswitch," *Journal of Microelectromechanical Systems,* June, **11** (3), pp. 276–283.

[26] Meier R. E., 1998, "DMD pixel mechanics simulation," *TI Technical Journal*, Special issue on DLP—DMD Manufacturing and Design Challenges, July–September, pp. 64–74.

[27] Nadal-Guardia R., Dehe A., Aigner R. and Castaner L. M; 2002, "Current drive methods to extend the range of travel of electrostatic microactuators beyond the voltage pull-in point," *Journal of Microelectromechanical Systems,* **11** (3), pp. 255–263.

[28] Nathanson H. C., Newell W. E., Wickstrom R. A. and Davis J. R., 1967, "The Resonant Gate Transistor", *IEEE Trans. on Electron Devices,*, **14** (3), pp. 117–133.

[29] Nemirovsky Y. and Bochobza-Degni O., 2001, "A Methodology for the Pull-In Parameters of Electrostatic Actuators," *Journal of Microelectromechanical Systems,* **10** (4), pp. 601–615.

[30] Ortega R., 1998, *Passivity-based control of Euler-Lagrange systems: mechanical, electrical and electromechanical applications,* Springer-Verlag, London.

[31] Ortega R., Van der Schaft A. J., Mareels I. and Maschke B., 2001, "Putting Energy Back in Control," *IEEE Control Systems Magazine*, April, pp 18-33.

[32] Pelesko J. A. and Triolo A. A., 2001, "Nonlocal Problems in MEMS Device Control," *J. of Enginering Mathematics* **41** (4), 345 – 366.

[33] Pelesko J. A., 2002, "Mathematical Modeling of Electrostatic MEMS with Tailored Dielectric Properties," *SIAM J. Appl. Math.* **62**, pp. 888-908.

[34] Sane H. S., Yazdi N. and Mastrangelo C. H., 2003, "Application of Sliding Mode Control to Electrostatically Actuated Two-Axis Gimbaled Micromirrors," *Proc. of the American Control Conference, Denver, CO*, June, pp. 3726–3721.

[35] Seeger J. I. and Crary S. B., 1997, "Stabilization of Electrostatically Actuated Mechanical Devices," *Proc. of the Ninth Int. Conf. on Solid-State Sensors and Actuators (Transducers '97)*, Chicago, IL, June 16-19, pp. 1133–1136.

[36] Seeger J. I. and Boser B. E., 1999, "Dynamics and Control of Parallel-Plate Actuators Beyond the Electrostatic Instability," *Proc. of the Tenth Int. Conf. on Solid-State Sensors and Actuators (Transducers '99)*, Sendai, Japan, June 7-9, pp. 474–477.

[37] Seeger J. I. and Boser B. E., 2003, "Charge Control of Parallel-Plate, Electrostatic Actuators and the Tip-In Instability," *Journal of Microelectromechanical Systems,* 12 (5), pp. 656–671.

[38] Sepulchre R., Jankovic M. and Kokotovic P., 1997, *Constructive Nonlinear Control,* Springer-Verlag, London.

[39] Senturia S. D., 2001, *Microsystem Design*, Kluwer Academic Publishers, Norwell, MA.

[40] Teel A. R., Kaiser O. E. and Murray R. M., 1997, "Uniting Local and Global Controllers for the Caltech ducted fan," *Proc. of the American Control Conference, Albuquerque, NM,* Jun 04-06, pp. 1539-1543.

[41] Toshiyoshi H., Mita M., Fujita H., 2002, "A MEMS Piggyback Actuator for Hard-Disk Drives," *J. of Microelectromechanical Systems*, **11** (6), pp. 648–654.

[42] Van der Schaft A. J., 2000, *L_2-Gain and Passivity Techniques in Nonlinear Control,* Springer-Verlag, London.

[43] Wang P. K. C., 1998, "Feedback Control of Vibrations in a Micromachined Cantilever Beam with Electrostatic Actuators", *Journal of Sound and Vibration*, **213** (3), pp. 537–550.

[44] Wonham W. M., 1985, *Linear Multivariable Control: A Geometric Approach*, 3^{rd} Edition, Springer-Verlag, New York.

[45] Yee Y., Nam H.-J., Le S.-H., Bu J. U., and Lee J.-W., 2000, "PZT Actuated Micromirror for Fine-Tracking Mechanism of High-Density Optical Data Storage" *Sensors and Actuators* **2864**, pp. 1-8.

[46] 2002 "Analyzing Hazards from a Distance", *Sandia Technology. a Quarterly Research and Development Journal, Fall,* **4** (3), pp. 11–12.